Optimal Design of a Renewable Energy System for an Off-Grid Desalination Facility on the Navajo Nation in the United States

Daming Xu
School of Mechanical Engineering
Xi'an University of Science and Technology
Xi'an, China
xu_daming@hotmail.com

Thomas L. Acker
Professor of Mechanical Engineering
Northern Arizona University
Flagstaff, Arizona, USA
Tom.Acker@nau.edu

***Abstract*– This paper presents the results of using a genetic algorithm (GA) to find the optimal configuration for an off-grid, renewable energy, reverse osmosis desalination system. Finding the lowest levelized cost of energy (LCOE) was the objective of the optimization. The GA showed that the configuration with the smallest LCOE was a hybrid wind+photovoltaic+diesel+battery system, with an LCOE of 0.5269 $/kWh. A general conclusion was that the "more hybrid" the energy system, the lower the LCOE, due to the complementarity of the wind and solar energy. If constrained to exclude a wind turbine, the GA found the best configuration to be photovoltaic+diesel+battery, with an LCOE just slightly higher than the optimal configuration with a wind turbine. Finally, because errors in the wind power prediction exist, a sensitivity study was conducted, leading to the conclusion that if the wind speed is uniformly 5% less than in the TMY3 wind data, then the photovoltaic+diesel+battery solution becomes optimal.**

Keywords - brackish water desalination, reverse osmosis, off-grid, renewable energy, optimal sizing, genetic algorithm

I. INTRODUCTION

Arizona is located in the desert southwest of the United States. The Navajo Nation is located in the Northeast corner of Arizona, where a large portion of the population live away the urban centers and in rural, undeveloped areas. In these remote areas, residents haul water from other locations due to low water availability and poor water quality of the many regional wells. In the Black Falls area of the Southwest Navajo Nation (SNN), there are about 100 homes spread across a large region. Residents in these homes transport potable water from remote watering stations, averaging 0.38 m^3 (100 gal) per capita. In hauling this water, residents drive an average of nearly 50 km per day incurring costs of 3 to 10 US$ per 0.38 m^3 of potable water [1]. This cost is about 10 to 25 times what people pay for water in the nearby community of Flagstaff, Arizona, (0.385 US$ per 0.38 m^3). Flagstaff is a small city (population < 100,000) located ~80 km away.

In the Black Falls area of the SNN, there are ample solar and wind energy resources proximate to brackish groundwater resources. The area is characterized as sparsely vegetated ranch land, with no trees (see Fig. 1). In order to investigate the feasibility of producing affordable potable water from brackish water wells, the Navajo Nation is working with the U.S. Bureau of Reclamation to create a small-scale experimental desalination facility powered by off-grid resources (the nearest connection to the electrical grid is over 15 km distant). The proposed experimental desalination facility has an initial goal to produce 0.38 m^3 of fresh water per day from brine pumped from a well that produces water with ~1,000 mg/L of dissolved minerals [2]. If successful in reliably producing potable water, the pilot facility will be scaled-up to fresh water production of 11.4 m^3/d (3,000 gal/d).

Figure 1. Desalination facility terrain view, looking northeast [2].

One desalination technology being considered for the experimental facility is reverse osmosis (RO). The purpose of this work was to find the optimal configuration for an off-grid, renewable energy (RE) system to power the RO desalination system. The RO system is assumed to run continuously, and therefore the objective function selected for the optimization was the lowest levelized cost of energy (LCOE). The capacity of the RO system was selected at 11.36 m^3/d (3000 gal/d), requiring a constant power consumption of 2.366 kW [3]. A renewable energy system simulation and genetic algorithm (GA) was used to determine the optimal configuration, implemented using the software MATLAB (https://www.mathworks.com/) [3]. The

'This research was supported in part by the Science Research Project (No. 16JK1506) of Education Department of Shaanxi Provincial Government, P. R. China, and in part by the Navajo Nation Department of Water Resources '

purpose of this paper is to describe the energy system simulation and optimization, to present its results, and to draw conclusions about the composition of the RE system. The energy system simulation implemented in the GA will be validated by comparison to a similar simulation using the commercial package HOMER (https://www.homerenergy.com/). Furthermore, the sensitivity of the optimal solution to errors in the wind speed will be investigated (i.e. will errors in the wind speed estimation change the optimal solution to include or exclude wind energy?).

II. Energy System Simulation

A. Off-grid RE system configuration

The first step in optimizing an energy system was to select the possible components of the system that are consistent with the local resources available. For the purpose of this analysis, the RE system could be composed of solar photovoltaic (PV) panels, small wind turbine generators (WTGs), diesel generators (DGs), a battery energy storage system (BESS), and associated inverters/converters. A schematic of the RE system with the RO connected to the AC bus is shown in Fig. 2.

B. Renewable Energy System Performance Simulation

To find the optimal configuration of the RE system, it was first necessary to develop a simulation of the energy system including performance models for the components and an algorithm for dispatch of the components. The simulation used an hourly timestep, and therefore solar and wind energy production was based upon hourly averages of the resources. Because a detailed description of the energy system modeling is presented in [3], only a summary is provided in the paragraphs that follow.

Solar radiation and wind speed data sets – Version three of the typical meteorological year data set (TMY3) was used to supply hourly average solar radiation and wind speed data for a one-year period [4]. TMY3 data from the location at Winslow, Arizona was chosen, since it is the site nearest to the location of the desalination facility among the locations available in the TMY3s (approximately 50 km from the desalination site). The TMY3 data for global horizontal radiation, diffuse horizontal radiation, extraterrestrial horizontal radiation, temperature and wind speed were employed, with the ground reflectance as 0.2. Wind speed is assumed to be at a height of 10 m [5] above the ground level (AGL). Wind speed can vary substantially across 50 km. To confirm the Winslow data is representative of the wind resource at the desalination site, the Arizona interactive wind map was consulted, showing that average wind speeds at 30-m AGL at both sites are within the same 0.5 m/s wind speed bin (http://sweetbriar.egr.nau.edu/website/windy/viewer.htm). The source data for the map is meso-scale weather modeling conducted by AWS TruePower (https://aws-dewi.ul.com/). Furthermore, both sites have similar topographical characteristics with no major changes in the terrain separating them.

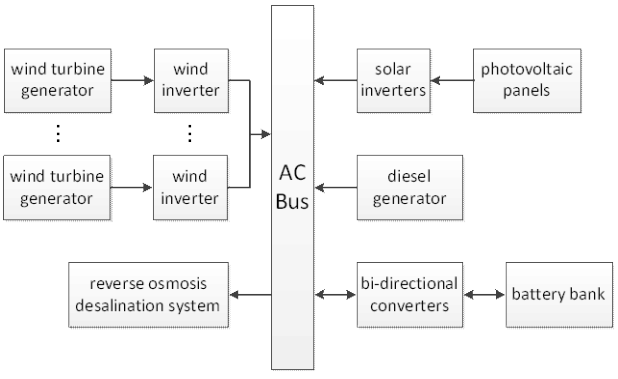

Figure 2. Schematic of the renewable energy system configuration [3].

Solar PV modeling – The solar PV considered in this model was assumed to be fixed-axis at a zero-azimuth angle, but could be tilted at any angle from 0° (horizontal) to 90° (vertical and facing south). The Hay-Davies-Klucher-Reindl anisotropic model was used to compute the total hourly incident irradiance on a tilted PV panel surface [6]. The total solar radiation consists of beam radiation and diffuse radiation from the sky, and ground-reflected radiation. To determine the average hourly output of the PV panels, the computational model in Lasnier and Gan Ang was used [7]. This model defines the current-voltage relationships based on PV panel electrical characteristics, including the effects of radiation level and panel temperature upon power output. The power output power was computed assuming maximum power point tracking.

Wind turbine modeling – The TMY3 average hourly wind speed data from the Winslow location was assumed to apply at the desalination site. This data is valid at 10-m above ground level, whereas a wind turbine installation at the desalination site will be at a 30-m hub height. To adjust the 10-m data to 30-m, a power-law relationship using the $1/7^{th}$ power law exponent for a turbulent boundary layer profile was used [8]. Because wind speeds can vary significantly with location, simulations will be conducted using the TMY3 wind speed data, and the TMY3 data uniformly adjusted by ±5% and ±10%, in order to provide an indication of the sensitivity of the LCOE and optimal system configuration to errors in the wind speed. The average wind power production for an hour is calculated by taking the TMY3 wind speed data, adjust it to a 30-m hub height, and then transforming it to power via the WTG power curve. The power curve relates the hub height wind speed to the power output of the turbine. Three different turbine models were considered, as described in a following paragraph.

Battery energy storage system modeling – For this initial investigation, lead-acid batteries were selected due to their long history of use and well understood cost and maintenance characteristics. To calculate battery lifetime, the Ampere-hour (Ah) counting model [12] was used along with the depth of discharge (DOD)-cycles to failure relations for general valve regulated lead acid (VRLA) batteries. For the Ah counting model, battery lifetime Ah throughput is obtained by multiplying the lifetime throughput coefficient with the rated Ah capacity. The mean lifetime Ah throughput was assumed to be the mean lifetime throughput coefficient multiplied by the rated Ah capacity. Strings of VRLA 200Ah, 2V batteries were used, with 24 batteries in series in one string, summing to 48 V per string. The mean lifetime throughput coefficient of the batteries was

587.5, thus the VRLA battery mean lifetime Ah throughput was 117,500 Ah. The batteries were assumed to have a round-trip efficiency of 0.85 and the DOD was set as 50% to avoid deep discharge that shortens their lives.

Diesel generator modeling and dispatch – In order to provide continuous power to the RO system, the power supplied by the intermittent wind and/or PV power needs to be coupled with a combustion engine, batteries, or both. For this study, a 5 kW Cummins Onan QD, quiet commercial mobile diesel generator was selected [9,10]. A 5 kW DG was selected so that it could be set to run at 50% to 75% of its rated power for fuel efficiency and mechanical health. When use of a DG was required, the RO system power consumption was about 50% of the DG rated power. For this simulation, the DG output was set at 75% of its rated capacity, a good load level for mechanical health while allowing the DG to both run the RO system and recharge the batteries. The engine filters for diesel oil, air and lubricant require replacement every 500 working hours [11]. The specific fuel consumption rate was derived from the engine specification sheet, and was approximately 0.26 L/h/kW.

To supply the electrical load, power resources are dispatched in the following order: 1) the WTGs and PV panels; 2) the batteries; and, 3) the DG [3,25], employing the micro-cycling dispatch strategy [26]. The DG starts when the battery state of charge (*SOC*) drops to a defined set point (SOC_{start}), and stops if the renewable energy production plus the battery bank can cover the load. Thus, the DG is dispatched to cover the load when there is insufficient energy produced by the wind and/or solar resources at the beginning of any time step *t*, and if the battery state of charge is insufficient, i.e. $SOC_t < SOC_{\text{start}}$ (in this modeling, SOC_{start} is 50%). In the following time step, if renewable energy plus the battery bank adequately covers the load and $SOC_t > SOC_{\text{start}}$, then the DG stops; otherwise, the DG keeps running. When the SOC_t is 100% and if there is excess renewable energy, the renewable power generation will be constrained.

In dispatching the batteries and/or DG in the energy system it is possible that during some hours of the year that the will be a loss of power supply (LPS) (note: when running the GA, it is possible that a candidate RE system will not have a DG, batteries, or both). The loss of power supply probability (LPSP) is then calculated by dividing the LPS by the total electrical energy load during the year. In such cases, the simulation sums the total energy deficit over the year. For any given candidate RE system, if the LPSP is above a predefined threshold, then the system configuration is discarded as an infeasible solution. For this simulation, the RO system is assumed to be running all the time, thus any RE system with an LPSP > 0 is discarded as infeasible.

C. RE Component Specifications

The solar inverters, wind inverters, and bi-directional converters (Fig. 1) were modeled using conversion efficiencies. The bi-directional converter working efficiency depends on its role as an inverter or rectifier. Table 1 shows the specifications for these components, along with the other RE equipment selected for use in this off-grid system.

Table 1. RE system components and specifications [3].

Energy System Component	Characteristics
Wind Turbine Generator: Tumo-Int [13]	
Type I: 1kW, 3-blade	$2,000
Type II: 2 kW, 3-blade	$4,000
Type 3: 3 kW, 5-blade	$5,000
Annual Maintenance	5% of capital
Lifetime	10 years
Wind Inverter: SMA Windy Boy [14,15]	$1/W
Efficiency	93%
Annual Maintenance	3% of capital
Lifetime	10 years
PV: SolarWorld SW270 Black Mono [16]	$290/panel
Max power	270 W
Module efficiency	16.1%
Annual Maintenance	3% of capital
Lifetime	20 years
Solar Inverter: SMA Sunny Boy [17,18]	$0.37/W
Efficiency	95%
Annual Maintenance	3% of capital
Lifetime	10 years
DG: Cummins Onan QD 5 kW [9,10,11]	$8,135
Rated power	5 kW
Filters cost (change every 500 h)	$50
Cost of diesel	$0.86/L
Annual Maintenance	5% of capital
Lifetime	10,000 h
VRLA Batt: Enersys PowerSafe OPzV [19,20]	$300/kWh
Rated capacity	200 Ah, 2V
Roundtrip efficiency	85%
Annual Maintenance	3% of capital
Lifetime - determined via lifetime curves [21,22]	
Bi-dir. Conv. (SMA Sunny Island) [23]	$0.7/W
Inverter efficiency	94.5%
Rectifier efficiency	98%
Annual Maintenance	3% of capital
Lifetime	10 years

D. Cost Function: Levelized Cost of Energy (LCOE)

The figure of merit upon which the RE systems are judged is the levelized cost of energy (LCOE). This, therefore, is the cost function that the GA minimizes in finding the optimal RE system. The equation for the LCOE is as follows [24]:

$$LCOE = \sum_{j=1}^{n} \frac{I_{P,j} + M_{P,j} + F_{P,j}}{(1+r)^j} \Big/ \sum_{j=1}^{n} \frac{E_j}{(1+r)^j} \quad (1)$$

where I_P, M_P and F_P represent the investment, maintenance and operations, and fuel costs of the RE system, E is the energy produced, and r is the discount rate. The discount rate and project lifetime, n, were assumed to be 3% and 10 years, respectively.

III. Genetic Algorithm Optimization

Based upon the principle of natural selection, a GA is a stochastic global search method. Similar to the process that that drives biological evolution, it does not require derivative or other auxiliary information. GAs can be used to solve both constrained and unconstrained optimization problems. The GA used in this work implemented the MATLAB functions available from the Genetic Algorithm Toolkit at The University of Sheffield, UK [27]. Fig. 3 shows an illustration of the flowchart and logic implemented in the GA employed in this work; for a detailed description, see [3]. The GA starts with a randomly generated initial population of feasible RE system configurations, composed of any combination of PV, WTGs, BESS, and a DG. Note, the RE system configuration can be constrained to include or exclude any component. For example, when running the GA, one can exclude a WTG if wanting to find the optimal solution in absence of an WTG, etc.

Each individual RE system configuration was identified using integer encoding. Thus, the population structure is given by:

$$population = \begin{bmatrix} g_{1,1} & g_{1,2} & \cdots & g_{1,L_{ind}} \\ g_{2,1} & g_{2,2} & \cdots & g_{2,L_{ind}} \\ \cdot & \cdot & \cdots & \cdot \\ g_{N_{ind},1} & g_{N_{ind},2} & \cdots & g_{N_{ind},L_{ind}} \end{bmatrix} \quad (2)$$

In this matrix, each row corresponds to an individual in the population, where an individual represents one possible configuration of the RE system. The elements in each row represent the decision variables that characterize that individual. For example, $g_{2,1}$ represents decision variable 1 in individual 2.

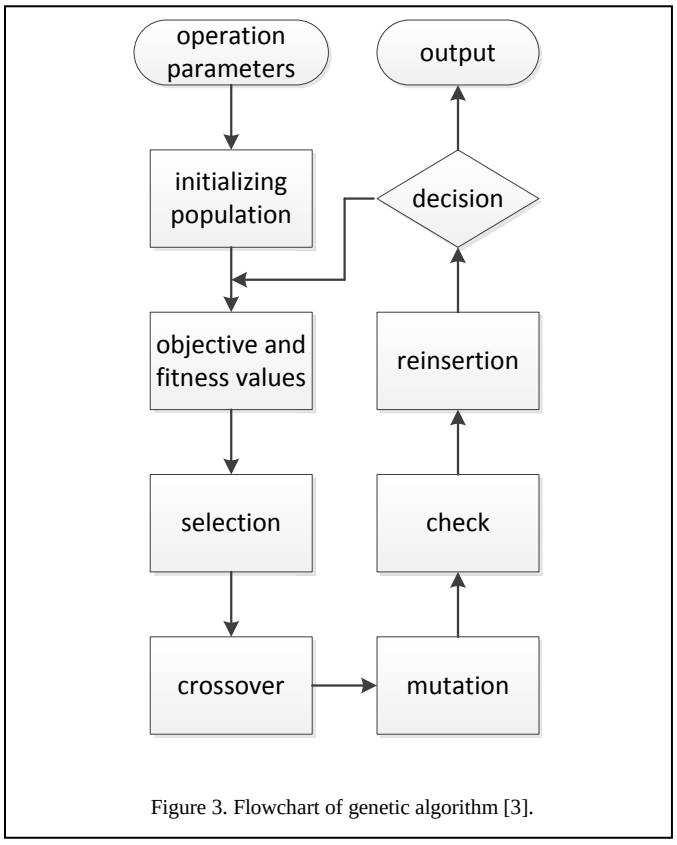

Figure 3. Flowchart of genetic algorithm [3].

N_{ind} and L_{ind} represent the number of individuals in a population and the number of decision variables per individual, respectively. The decision variables of an individual were sequenced in the following order: [$Type_{WTG}$ N_{WTG} β $N_{PV,p}$ $N_{batt,p}$ N_{DG}], representing the type of WTG, the number of WTGs, the tilt angle (β) of the PV, the number of strings of PV in parallel, the number of battery strings in parallel, and the number of DGs. For this simulation, the inverters and convertors were selected as 48V DC. In order to match this 48V input required three PV panels connected in series on one string, and 24 2V batteries connected in series in one string. After a population of individuals is created, each individual is run through the simulation to determine its performance over 8760 hours. The LPSP of every individual is calculated, and inspected to see if LPSP > *0*. The refusal strategy was used, and individuals not up to grade are rejected and new individuals are created and checked until the population is formed.

When implemented, the GA commences evaluating the LCOE and ranking the fitness of the candidate RE systems in the initial generation. It then evolves a new generation of candidates, evaluates and ranks their fitness, evolves a new generation, and so on, until it approaches the optimal solution. It is fairly easy to see when the optimal solution is achieved by plotting the smallest LCOE from each generation; when the LCOE becomes unchanging from generation to generation, the optimal solution has been found. In this work, that normally happened in less than 1,000 generations.

IV. Results

A. Simulation Validation with HOMER

Prior to running the GA to find the optimal solution, several checks were made of the simulation program to ensure it was accurately computing the output of each energy system component and dispatching the system appropriately. One comparison was to perform an energy simulation for an RE configuration where each energy system component is present, and compare it to the energy simulation performed by HOMER for a system with the same components and specifications. The results of a comparison for system configuration [II 3 35° 6 1 1] is shown in Table 2 (three type II WTGs, 6 strings of PV panels tilted at 35°, 1 string of batteries, and 1 DG). As can be seen, the simulations yield similar energy outputs for each component [3]. The most significant difference is in the

Table 2. Comparison of energy simulation results to that using HOMER, for the following RE system configuration: [II 3 35° 6 1 1] [3].

	Homer	Simulation program	Deviation from Homer (%)
PV (kWh/y)	10,582	10,306	-2.6
WTG (kWh/y)	12,001	11,124	-7.3
DG (kWh/y)	7,974	7,995	0.3
DG operation hour (Hour/y)	2,130	2,132	0.1
Diesel consumption (L/y)	3,941	4,037	2.4
Battery Ah throughput (kWh/y)	4,486	4,415	-1.6
*PV and wind energy generated was measured on the AC bus.			

generation by the WTGs, which is due to different methods/data for calculating the output.

B. Results of Genetic Algorithm Optimization

Executing the GA using the TMY3 data and RE system components described earlier resulted in the following individual having the lowest LCOE of 0.5269 $/kWh: [II 2 25° 6 1 1]. Therefore, this RE configuration was identified as the best solution [3]. In words, this individual RE system was composed of two 2-kW type II WTG, six strings of PV panels (therefore a total of 18 PV panels) at a tilt angle of 25°, one string of batteries and one DG. As mentioned previously, when running, the DG was set to 75% of its rated power, 3.75 kW. Since the RO load was 2.366 kW, the remaining 1.384 kW could be utilized to charge the battery bank. For this optimal solution, the charging current was about 28.3 A after rectifiers, which is 0.14 C for a battery string. A charging current less than 0.2 C is considered good [25], and therefore the DG rated power selection is appropriate.

C. Comparison of LCOE for Constrained RE Configurations

Fig. 4 shows an LCOE comparison of the optimal solutions found by the GA for seven power system configurations, numbered 'a' to 'g'. Except for configuration 'a', where any energy system component was permitted, each configuration only permitted the components identified in the legend. For example, in configuration 'b' a WTG was not permitted, in configuration 'f' neither PV nor WTGs were permitted, etc. When comparing each of these configurations, it can be seen that the configuration with the lowest LCOE at $0.5269 $/kWh was 'wind/PV/DG/battery' with its optimal solution [II 2 25° 6 1 1]. The configuration with the next lowest LCOE was 'b' [- - 34 6 1 1] with an LCOE of 0.5344 $/kWh. Looking at configurations 'c' and 'd', both show a fairly significant increase in LCOE compared to 'a' and 'b'. Indeed, a general conclusion from the results in Fig. 4 is that the "more hybrid" the configuration, the lower the LCOE. Looking in-depth at the energy production profiles, it appears that this is due to the wind and solar resources having different and complementary production patterns, leading to a lower LCOE.

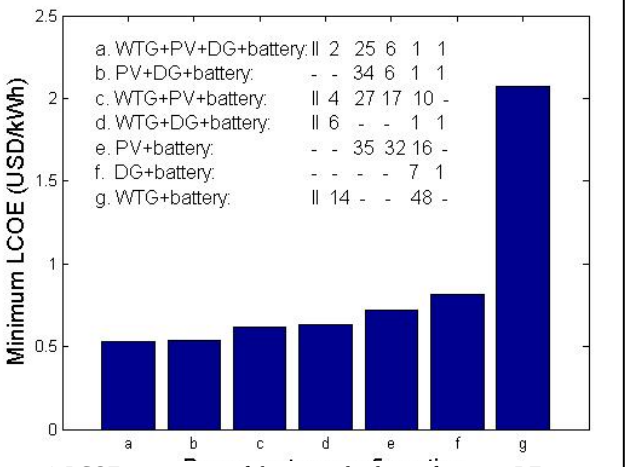

Figure 4. LCOE comparison of the optimal solution for seven RE system configurations.

D. Sensitivity of Optimal Solution to Errors in the Wind Speed

One observation of the simulation energy output comparison shown in Table 2 was that the wind energy production was over 7% different between the current simulation and HOMER. Because TMY3 data used in the simulation is distant from the site, it is likely that the wind power production will be different that predicted. To investigate the effect on LCOE and optimal solution of differences between the TMY3 wind speed data and that actually available at the desalination site, a sensitivity study was conducted. The TMY3 hourly average wind speed data was modified by ±5% and ±10% for each hour of the year, and the GA optimization was repeated. The LCOE results for the optimal configurations in each of these cases are shown in Fig. 5. Referring to the horizontal axis, for a multiple of '1', the best solution is the one presented previously: [II 2 25° 6 1 1] with 0.5269 $/kWh. If decreasing the TMY3 wind speed by 5% (thus a multiple of 0.95), the best solution is now PV/DG/battery [- - 34 6 1 1] with an LCOE of 0.5344 $/kWh, the same presented in Fig. 4. Note in this case (TMY3 multiplier of 0.95), the best solution for a configuration with WTG/PV/DB/battery is still [II 2 25° 6 1 1], but the LCOE has risen to 0.5399 $/kWh, so just above the PV/DG/battery solution. Thus, the crossover point for choosing between these two configurations occurs at a multiple very near 0.95. For further decreases in the wind speed (multiple of 0.9), the optimal configuration remains PV/DG/battery. Considering the case where the wind speed is higher at the desalination site, referring to multipliers of 1.05 and 1.10 in Fig. 5, the best configuration is still identified as WTG/PV/DG/battery [II 2 25° 6 1 1] with significant (about 1%) drops in the LCOE.

V. CONCLUSIONS

The purpose of this work was to find the optimal configuration for a renewable energy, off-grid, reverse osmosis desalination system using a genetic algorithm, where the

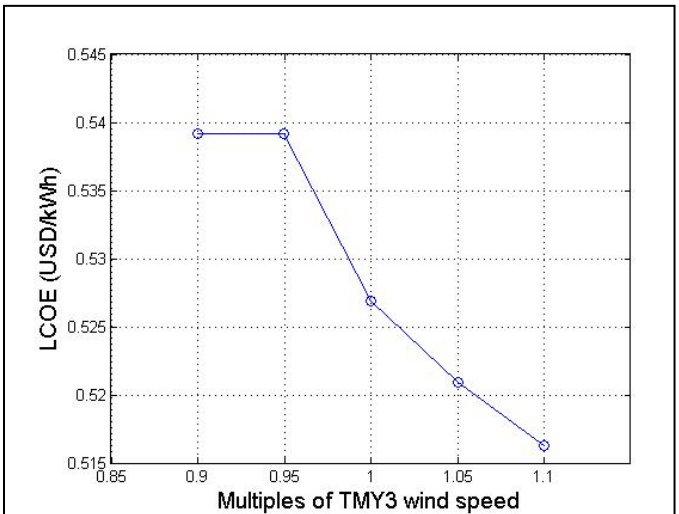

Figure 5. LCOE for optimal solution versus multiplier for the TMY3 hourly average wind speeds.

objective was to find the system configuration with the lowest levelized cost of energy. The RO system capacity was a design constraint, and set at 11.36 m^3/d (3000 gal/d). Its electric power consumption was assumed constant and equal to 2.336 kW (i.e. it was not dispatchable and would run constantly, and not be started and stopped on a daily basis). The results of the GA found the lowest LCOE of 0.5269 $/kWh for a system configuration with two 2-kW type II WTG, six strings of PV panels (18 PV panels) at a tilt angle of 25°, one string of batteries and one DG [II 2 25° 6 1 1]. A general conclusion was that the "more hybrid" the energy system, the lower the LCOE, due to the complementarity of the wind and solar energy. If constrained to exclude a WTG, the GA found the best configuration to be PV/DG/battery, with an LCOE just slightly higher than the optimal configuration with a WTG. Finally, because errors in the wind speed and wind power prediction exist, a sensitivity study was conducted, leading to the conclusion that if the wind speed is uniformly 5% less at the desalination site than in the TMY3 data, then the PV/DG/battery solution becomes optimal.

ACKNOWLEDGMENTS

In addition to the Shaanxi Provincial Government, P. R. China, and the Navajo Nation, the authors wish to acknowledge and thank The University of Sheffield and the creators of the GA Toolbox for making their code freely available.

REFERENCES

[1] Haws, M. "Solar Desalination Using Distillation," USBR, Res. Dev. Off. Sci. Technol. Program, Final Rep. 2014, Proj. ID 4850, 2015.

[2] Guerrero, J.D.A., "Wind Power Modeling for a Rural Desalination Project," M.S. Thesis, Northern Arizona University, 2016.

[3] Xu, D., and T. L. Acker, "Optimal sizing of an off-grid, renewable energy reverse osmosis desalination system based on a genetic algorithm," J. Desalination and Water Treatment, in press.

[4] Wilcox, S. and W. Marion, Users Manual for TMY3 Data Sets, NREL/TP-581-43156, May 2008.

[5] Huld, T., Paietta, E., Zangheri, P., and I.P. Pascua, "Assembling Typical Meteorological Year Data Sets for Building Energy Performance Using Reanalysis and Satellite-Based Data," *Atmosphere* 2018, 9(2), 53; doi:10.3390/atmos9020053.

[6] Duffie, J.A. and W.A. Beckman, Solar engineering of thermal processes, Wiley, 2013.

[7] Lasnier, F. and T. Gan Ang, Photovoltaic engineering handbook, A. Hilger, ISBN 0-85274-311-4, IOP Publishing Ltd 1990.

[8] Borowy, B.S., and Z.M. Salameh, "Methodology for optimally sizing the combination of a battery bank and PV array in a wind/PV hybrid system," IEEE Trans. Energy Convers. 11 (1996) 367–375. doi:10.1109/60.507648.

[9] Commercial generator set Quiet Diesel TM Series QD 5000. https://powersuite.cummins.com/PS5/PS5Content/SiteContent/en/Binary_Asset/pdf/Consumer/specsheets/a-1452.pdf (accessed January 20, 2019).

[10] Cummins Onan 5 HDKBC-2860 QD 5000 - 5000 Watt Quiet Diesel Commercial Mobile Generator 120V 25A. https://www.electricgeneratorsdirect.com/Cummins-Onan-5-HDKBC-2860/p15742.html (accessed January 20, 2019).

[11] Emergency Power, 10,000 Watt Home Diesel Generator. https://www.auroragenerators.com/products/10kw-home-diesel-generator (accessed February 5, 2019)

[12] Farret, F.A., and M.G. Simões, Integration of alternative sources of energy, IEEE Press, 2006.

[13] Tumo Int Corporation Limited, Tumo-Int Wind Turbine Generators. http://tumo-int.com/product.php (accessed January 20, 2019).

[14] Windy Boy 5000 Windy Boy 6000 Inverter for Wind Energy Power Plants Operating Instructions, n.d. http://files.sma.de/dl/5661/WB50_60-11-FE4105.pdf.

[15] SMA Windy Boy 5000-US 5KW Wind Inverter SB 5000US WB - Solaris. https://www.solaris-shop.com/sma-windy-boy-5000-us-5kw-wind-inverter-sb-5000us-wb/ (accessed January 20, 2019).

[16] SolarWorld SW270 Black Mono Solar Panel - Wholesale Solar. https://www.wholesalesolar.com/1922269/solarworld/solar-panels/solarworld-sw270-black-mono-solar-panel (accessed January 20, 2019).

[17] Solar Inverters. www.sma-america.com/products/solarinverters.html (accessed January 20, 2019).

[18] SMA Sunny Boy 5.0-US Inverter - Wholesale Solar. https://www.wholesalesolar.com/2931725/sma/inverters/sma-sunny-boy-5.0-us-inverter (accessed January 20, 2019).

[19] PowerSafe OPzV Batteries. http://www.enersys-emea.com/reserve/pdf/EN-PS-OPzV-RS-004_0414.pdf (accessed Feb 5, 2019).

[20] O'Connor, J.P., Off Grid Solar: A handbook for Photovoltaics with Lead-Acid or Lithium-Ion batteries, ISBN 1537622617, 2016.

[21] Wust, R., "Hybrid power system model how to get the most from your system," in: Intelec 2012, IEEE, 2012: pp. 1–8. doi:10.1109/INTLEC.2012.6374499.

[22] Drouilhet, S., and B.L. Johnson, A Battery Life Prediction Method for Hybrid Power Applications Preprint Work performed under task number WE712360, NREL/CP-440-21978. (1997).

[23] SMA Sunny Island 5048U 5KW Battery Inverter SI 5048U - Solaris. https://www.solaris-shop.com/sma-sunny-island-5048u-5kw-battery-inverter-si-5048u/ (accessed January 20, 2019).

[24] U.S. Department of Energy, "Levelized Cost of Energy (LCOE)," www.energy.gov/sites/prod/files/2017/12/f46/levelized-cost.pdf (accessed January 7, 2019).

[25] Xu, D. and L. Kang, "Optimal dispatch of unreliable electric grid-connected diesel generator-battery power systems," Int. J. Emerg. Electr. Power Syst. 16 (2015). doi:10.1515/ijeeps-2014-0130.

[26] Bernal-Agustín, J.L., and R. Dufo-López, "Simulation and optimization of stand-alone hybrid renewable energy systems," Renew. Sustain. Energy Rev. 13 (2009) 2111–2118. doi:10.1016/J.RSER.2009.01.010.

[27] Chipperfield, A., Fleming, P., Pohlheim, H., and C. Fonseca, "Genetic Algorithm Toolbox User's Guide Version 1.2," n.d., http://codem.group.shef.ac.uk/index.php/ga-toolbox, accessed April 2019.